

# Many-body aspects of positron annihilation in the electron gas

V. Apaja, S. Denk, and E. Krotscheck

*Institut für Theoretische Physik, Johannes Kepler Universität, A 4040 Linz, Austria*

## Abstract

We investigate positron annihilation in the electron gas as a case study for many-body theory, in particular the optimized Fermi Hypernetted Chain (FHNC-EL) method. We examine several approximation schemes and show that one has to go up to the most sophisticated implementation of the theory available at the moment in order to get annihilation rates that agree reasonably well with experimental data. Even though there is basically just one number we look at, the electron-positron pair distribution function at zero distance, it is exactly this number that dictates how the full pair distribution behaves: In most cases, it falls off monotonously towards unity as the distance increases. Cases where the electron-positron pair distribution exhibits a dip are precursors to the formation of bound electron-positron pairs. The formation of electron-positron pairs is indicated by a divergence of the FHNC-EL equations; from this we can estimate the density regime where positrons must be localized. This occurs in our calculations in the range  $9.4 \leq r_s \leq 10$ , where  $r_s$  is the dimensionless density parameter of the electron liquid.

PACS numbers: 78.70.Bj, 71.10.Ca

## I. INTRODUCTION

The process of electron–positron annihilation has been studied intensively for several decades. In recent years positron annihilation spectroscopy has been routinely used for studying the electronic structures of solids. As far as the two–body process is concerned, the appropriate theoretical framework is quantum–electrodynamics (QED). Differential cross sections and annihilation rates have been examined for two–particle systems like positronium in much detail, and can be found in standard textbooks [1, 2]. Coincidence measurements of gamma emission give the angular correlation of annihilation radiation (ACAR), that yields information about the electron momenta. As the recent discovery of the electronically stable bound positron-Li state showed [3], positrons in contact with neutral atoms can also be an interesting few–body system. Since then the list of atoms binding positrons has become long; the underlying calculations are usually performed using either the stochastic variational method or the configuration integration method.

Annihilation of positrons in matter adds a many–body aspect to the problem. The experimental annihilation rates are by now well established, we shall compare our results with the data measured by Weisberg and Berko [4] for alkali metals. In his pioneering work, Ferrell [5] gives intuitive formulas for the annihilation rates. The simplest “many–body” methods use single particle wave functions; in this case, the only true many–body effect is the Pauli exclusion principle acting between electrons, but *many–body correlations* between the interacting particles are *not* taken into account. Qualitatively, correlations can be introduced by applying enhancement factors as described by Brandt [6]. A popular method for electron structure calculations and potentially also for positron systems [7] is density functional theory (DFT). In particular, there are numerous applications of DFT to defects in solids. In DFT one can write the annihilation rate in terms of the electron and positron densities, and an enhancement factor [8] to account for the excess electron density near the positron, in other words, to describe electron–positron correlations.

The enhancement factor has been the subject of many recent studies [9, 10, 11]. Once the enhancement factor is known, one can apply standard DFT under various approximate schemes, like the local density approximation (LDA), generalized gradient approximation (GGA) or the weighted density approximation (WDA). One can then also evaluate the partial annihilation rates due to valence and core electrons. The density functionals are

derivatives of known properties of electron gas or electron–positron mixtures, and their quality has been tested only in the case of a positron–neutral atom bound system [11]. So far there have not been many attempts to formulate a microscopic many–body theory that deals with an *inhomogeneous* electron gas. A first move to this direction was made by Stachowiak and Boroński [12], who studied the case of a spherical inhomogeneity in jellium.

Most of the many–body aspects of positron annihilation rates are reflected in a single number, namely the value of the electron–positron distribution function,  $g^{\text{IB}}(r)$ , at the origin. (As a convention, we shall label all two–body quantities that involve one positron (“impurity”) and one electron (“background”) with a superscript IB.) The annihilation rate of a positron in *homogeneous* electron gas can be written in the form [13],

$$\frac{1}{\tau} = \frac{12}{r_s^3} g^{\text{IB}}(0) \times 10^9 \text{sec}^{-1}, \quad (1.1)$$

where  $r_s$  is the familiar dimensionless density parameter of the electron gas. The  $r_s$ –factor in formula (1.1) is merely a geometric factor that takes into account the decreasing probability of finding an electron at the locations of the positron due to decreasing electron density. The “enhancement factor”  $g^{\text{IB}}(0)$  accounts for electron–positron correlations. These can be strong in a metal, hence  $g^{\text{IB}}(0)$  can be large. The positron impurity is delocalized at low  $r_s$  and cannot give rise to any appreciable local enhancement of the electron density. Instead, there is an increased probability of finding an electron near the positron: This tendency is visible only in the pair correlations, not in the density. This explains why annihilation rates computed using a *homogeneous* electron gas agree well with the experimental data up to  $r_s \sim 5$ . On the other hand, the electron density enhancement around a localized positron can be included, for example, in the spirit of LDA in DFT, where the electron–positron distribution function computed for the homogeneous case is multiplied with the spatially varying electron density [14, 15, 16].

The calculation of  $g^{\text{IB}}(r)$  is a matter of many–body physics, and the problem of determining  $g^{\text{IB}}(0)$  is evidently an issue of *short–ranged* correlations. Quite appropriately, it was dealt with within perturbation theory by solving the electron–positron Bethe–Goldstone equation [8]. Brown, Jackson, and Lowy [17, 18] have also examined short–ranged electron–electron correlations in a Bethe–Goldstone theory and pointed out the possibility of electron–positron pair formation at low electron densities (large  $r_s$ ). The theory of positron annihilation has been developed further by Boroński, Szotek and Stachowiak [19] and Rubaszek and Sta-

chowiak [20, 21], and it appears to be able to reproduce the observed annihilation rates in simple metals.

With the advent of highly re-summed variational techniques, a new generation of calculations containing vastly richer diagrammatic structures than Bethe–Goldstone calculations was possible. As a physically relevant paradigm for a fermion mixture and electron–hole liquids, positronic impurities and electron–positron mixtures have been studied quite extensively. Kallio, Pietiläinen and Lantto [22, 23] used the so-called “quasi-boson” approximation for the wave function of the electronic background, which maps the formalism to an effective boson theory. Closest to our approach are the calculations by Lantto [24] and Saarela [25]. Compared with the former one, the present work has an improved diagrammatic summation and in particular a more consistent treatment of the antisymmetry of the wave function. Lantto [24] also employs a simplified version of the Euler equation which corresponds to our FHNC//0 approximation to be discussed in section IV A, but the energy and the structure functions are evaluated using the full FHNC equations and thus violates the identities (2.14), (2.24) and (3.6). Saarela [25] modified the Euler–Lagrange equation of the pair-distribution function of a charged *Bose* system by adding an *ad hoc* electron–electron potential, such that the equation reproduces the exact free-fermion distribution in the limit of infinite density. Although oversimplified and phenomenological, this approach gives  $g^{\text{IB}}(0)$  close to the values obtained by Stachowiak and Lach [26] and Boroński and Nieminen [14]. Stachowiak *et al.* have used HNC theory in combination with a Hartree–Fock–type approximation and a self-consistent perturbation of a Jastrow state [27, 28, 29, 30, 31].

The present work should be considered as an exercise in basic microscopic many-body techniques. We shall first outline the most complete version of the optimized Fermi–hypernetted–chain theory (FHNC–EL) [32]. We will pay special attention to the full functional optimization of correlation functions, which removes all ambiguity from the optimization process. The technical details of our theory for a one-component electron system are described in Ref. 33, a more recent application to  $^3\text{He}$  which includes the optimization of triplet correlations and the calculation of proper elementary diagrams may be found in Ref. 34. We have also recently examined a completely analogous problem in helium liquids, namely the calculation of properties of  $^4\text{He}$  impurities in  $^3\text{He}$  [35]. We shall then discuss the impurity theory and derive the relevant Euler equations. In the following sections, we

will lead the reader through a sequence of plausible approximations in order to determine what it takes to get the physics right. We will show that the very simple approximation of a mixture of charged bosons gives a reasonably good agreement with experimental data. However, a bosonic theory is unsatisfactory *per se*, but it turns out that the first fermionic corrections make things worse and the agreement is lost. Finally, we will show that only the full fermion theory produces results which agree again with experimental data.

## II. OPTIMIZED FERMI HYPERNETTED CHAIN METHOD

### A. Variational Wave Function

This section gives a brief survey of the variational theory of a bulk Fermi liquid; the reader is referred to Refs. 33, 34 for details of the theory, and the diagrammatic definition of all technical quantities. Since no confusion can arise for the time being, we will in this section not spell out the particle species.

The Jastrow–Feenberg theory [36] for a Fermi liquid assumes a trial wave function of the form

$$\Psi_0(1, \dots, N) = F(\mathbf{r}_1, \dots, \mathbf{r}_N) \Phi_0(1, \dots, N), \quad (2.1)$$

$$F(\mathbf{r}_1, \dots, \mathbf{r}_N) = \exp \frac{1}{2} \left[ \sum_{1 \leq i < j \leq N} u_2(\mathbf{r}_i, \mathbf{r}_j) + \sum_{1 \leq i < j < k \leq N} u_3(\mathbf{r}_i, \mathbf{r}_j, \mathbf{r}_k) + \dots \right]. \quad (2.2)$$

$\Phi_0(1, \dots, N)$  is a model wave function, normally a Slater–determinant of plane waves. The *correlation functions*  $u_n(\mathbf{r}_1, \dots, \mathbf{r}_n)$  are made unique by imposing the *cluster-property*

$$u_n(\mathbf{r}_1, \dots, \mathbf{r}_n) \rightarrow 0 \quad \text{as} \quad |\mathbf{r}_i - \mathbf{r}_j| \rightarrow \infty. \quad (2.3)$$

The wave function (2.2) is not exact; one way to see this is by realizing that the nodes of the wave function (2.2) are identical to those of the model function  $\Phi_0(1, \dots, N)$ . In the parlance of Monte Carlo simulations this would be called a fixed node approximation.

### B. Fermion HNC equations

Two components are essential for the execution of the Jastrow–Feenberg variational theory: The first is the development of cluster–expansion and resummation methods for the

pair distribution function in the homogeneous case,

$$g(r) = \frac{N(N-1)}{\rho^2} \frac{\int d^3r_3 \dots d^3r_N |\Psi_0(1, \dots, N)|^2}{\int d^3r_1 \dots d^3r_N |\Psi_0(1, \dots, N)|^2}, \quad (2.4)$$

where  $r = r_{12} = |\mathbf{r}_1 - \mathbf{r}_2|$ ; spin-summations are tacitly implied. The second component of the theory is the *optimization* of the correlation functions by minimization of the total energy

$$\frac{\delta}{\delta u_n(\mathbf{r}_1, \dots, \mathbf{r}_n)} \frac{\langle \Psi_0 | H | \Psi_0 \rangle}{\langle \Psi_0 | \Psi_0 \rangle} = 0 \quad (2.5)$$

for the Hamiltonian

$$H = - \sum_{i=1}^N \frac{\hbar^2}{2m} \nabla_i^2 + \sum_{1 \leq i < j \leq N} v(|\mathbf{r}_i - \mathbf{r}_j|) \quad (2.6)$$

where, in our case  $v(r) = e^2/r$  is the Coulomb interaction.

Let us first turn to the pair distribution function  $g(r)$ , specifically to the FHNC equations determining  $g(r)$  from a given pair correlation function  $u_2(r)$ . Pair correlations are the most important ones, and in the case of electrons one usually neglects triplet correlations altogether. Justification for this stems from the study of triplet correlations in the 2D and 3D charged Bose gas [37] and verified by Monte Carlo calculations [38], note that triplet correlations are *not* the same as propagator corrections [34] which have occasionally been confused with Feynman–Cohen backflow.

The FHNC equations are a set of four configuration–space, and four momentum–space equations formulated in terms of “nodal”  $N_{ij}(r)$  and “non-nodal” diagrams  $X_{ij}(r)$  that are, in turn, characterized by their exchange structure  $\{ij\} \in \{dd, de, ee, cc\}$ . Input to the equations is the pair correlation function  $u_2(r)$ , the Slater exchange function  $\ell(x) = 3(\sin x - x \cos x)/x^3$ , and a set of “elementary diagrams”  $E_{ij}(r)$  [39] that must be calculated one by one.

The coordinate–space equations are

$$\begin{aligned} \Gamma_{dd}(r) &= X_{dd}(r) + N_{dd}(r) \\ &= \exp[u_2(r) + N_{dd}(r) + E_{dd}(r)] - 1, \\ X_{de}(r) &= [1 + \Gamma_{dd}(r)] [N_{de}(r) + E_{de}(r)] - N_{de}(r), \\ X_{ee}(r) &= [1 + \Gamma_{dd}(r)] \left[ -\frac{1}{\nu} L^2(r) + N_{ee}(r) + E_{ee}(r) \right] - N_{ee}(r) \\ &\quad + [1 + \Gamma_{dd}(r)] [N_{de}(r) + E_{de}(r)]^2, \\ X_{cc}(r) &= -\frac{1}{\nu} \Gamma_{dd}(r) L(r) + E_{cc}(r) \end{aligned} \quad (2.7)$$

where  $\nu$  is the degree of degeneracy of the single-particle states,  $L(r) = \ell(k_F r) - \nu [N_{cc}(r) + E_{cc}(r)]$ , and  $k_F$  is the Fermi wave number. The “nodal” quantities  $N_{ij}(r)$  are constructed in momentum space according to

$$\begin{aligned}\tilde{N}_{dd}(k) &= \frac{\tilde{X}_{dd}(k)}{[1 - \tilde{X}_{de}(k)]^2 - [1 + \tilde{X}_{ee}(k)] \tilde{X}_{dd}(k)} - \tilde{X}_{dd}(k), \\ \tilde{N}_{de}(k) &= \frac{1 - \tilde{X}_{de}(k) - \tilde{X}_{dd}(k)}{[1 - \tilde{X}_{de}(k)]^2 - [1 + \tilde{X}_{ee}(k)] \tilde{X}_{dd}(k)} - 1 - \tilde{X}_{de}(k), \\ \tilde{N}_{ee}(k) &= \frac{\tilde{X}_{dd}(k) + 2\tilde{X}_{de}(k) + \tilde{X}_{ee}(k) - 1}{[1 - \tilde{X}_{de}(k)]^2 - [1 + \tilde{X}_{ee}(k)] \tilde{X}_{dd}(k)} + 1 - \tilde{X}_{ee}(k), \\ \tilde{N}_{cc}(k) &= -\tilde{X}_{cc}(k) \left[ \frac{\tilde{l}(k)/\nu - \tilde{X}_{cc}(k)}{1 - \tilde{X}_{cc}(k)} \right].\end{aligned}\tag{2.8}$$

We have above used the convention of defining a dimensionless Fourier-transform as  $\tilde{f}(k) \equiv [f(r)]^{\mathcal{F}}(k) \equiv \rho \int d^3r f(r) e^{i\mathbf{k}\cdot\mathbf{r}}$ .

The pair distribution function can then be constructed from the above quantities:

$$g(r) = [1 + \Gamma_{dd}(r)] \left\{ -\frac{1}{\nu} L^2(r) + N_{ee}(r) + E_{ee}(r) + [1 + N_{de}(r) + E_{de}(r)]^2 \right\}.\tag{2.9}$$

The static structure function is equally important than the pair distribution function and has the relatively simple form

$$\begin{aligned}S(k) &= 1 + [g(r) - 1]^{\mathcal{F}}(k) \\ &= \frac{1 + \tilde{X}_{ee}(k)}{[1 - \tilde{X}_{de}(k)]^2 - [1 + \tilde{X}_{ee}(k)] \tilde{X}_{dd}(k)}.\end{aligned}\tag{2.10}$$

For further reference, we also introduce the quantity

$$S_d(k) = \frac{1 - \tilde{X}_{de}(k)}{[1 - \tilde{X}_{de}(k)]^2 - [1 + \tilde{X}_{ee}(k)] \tilde{X}_{dd}(k)},\tag{2.11}$$

and note the relationship

$$\tilde{\Gamma}_{dd}(k) = \frac{\tilde{X}_{dd}(k)}{[1 - \tilde{X}_{de}(k)]^2 - [1 + \tilde{X}_{ee}(k)] \tilde{X}_{dd}(k)}.\tag{2.12}$$

The representation (2.9) of  $g(r)$  contains an explicit factor

$$1 + \Gamma_{dd}(r) = \exp [u_2(r) + N_{dd}(r) + E_{dd}(r)].\tag{2.13}$$

This form is therefore the natural choice when working in coordinate space and focusing on the strong short-range correlation structure. On the other hand, when we consider the static structure function  $S(k)$ , the expression (2.10) is the more useful one.

The naïve implementation [40, 41] of the FHNC equations, referred to as FHNC//0 approximation, would suggest, in analogy to the boson theory, to start with the omission of the “elementary diagrams”  $E_{ij}(r)$  and include these, order by order, as *quantitative* improvements as the theory is moved to the next level. In the FHNC//n approximation one keeps “elementary” diagrams up to the  $n$ -point diagram. However [32], such a procedure violates the exact features

$$\begin{aligned}\tilde{X}_{\text{de}}(k) &= \mathcal{O}(k) & \text{as } k \rightarrow 0^+, \\ 1 + \tilde{X}_{\text{ee}}(k) &= S_{\text{F}}(k) + \mathcal{O}(k^2) & \text{as } k \rightarrow 0^+.\end{aligned}\tag{2.14}$$

These properties originate from the Pauli principle and are particularly important for the optimization problem [42]. They imply the cancellation of “elementary” and “non-elementary” exchange diagrams; in other words there exist classes of so-called “elementary” exchange diagrams that must not be neglected. We have dealt with these diagrams in an approximate way, dubbed as “//C”-approximation, which has been described and justified in Ref. 34.

### C. Background Energy calculation

The first step in deriving the Euler equations is the calculation of the energy functional. An important manipulation is the use of the *Jackson-Feenberg* identity

$$F\nabla^2 F = \frac{1}{2}(\nabla^2 F^2 + F^2\nabla^2) + \frac{1}{2}F^2[\nabla, [\nabla, \ln F]] - \frac{1}{4}[\nabla, [\nabla, F^2]],\tag{2.15}$$

which shows that the expectation value of the kinetic energy can be divided into three parts,

$$\langle \hat{T} \rangle = T_{\text{F}} - \frac{N\hbar^2\rho}{8m} \int d^3r g(r) \nabla^2 u_2(r) + T_{\text{JF}}.\tag{2.16}$$

Here  $T_{\text{F}}$  is the kinetic energy of the free Fermi gas, and  $T_{\text{JF}}$  is a kinetic energy term that is solely due to exchanges. We can write this term as

$$T_{\text{JF}} \equiv \frac{\hbar^2}{8m} \sum_i \frac{\langle \Phi_0 | [\nabla_i, [\nabla_i, F^2]] | \Phi_0 \rangle}{\langle \Phi_0 | F^2 | \Phi_0 \rangle} \equiv \frac{\hbar^2 N}{8m} \int d^3r \nabla_\ell^2 \rho_1(\mathbf{r}).\tag{2.17}$$

With  $\nabla_\ell$  we mean (indicated by the subscript  $\ell$ ) a gradient operator that acts on the Slater determinant only. Operationally, Eq. (2.17) is to be understood as follows: First one calculates — disregarding the fact that the density is uniform — a cluster expansion



of the one-body density  $\rho_1(\mathbf{r})$ . The operator  $\nabla_\ell^2$  then differentiates *the exchange lines only* that are attached, in such a cluster expansion, to the external point. This replaces the incoming and outgoing exchange lines  $\ell(|\mathbf{r} - \mathbf{r}_i| k_F) \ell(|\mathbf{r} - \mathbf{r}_j| k_F)$  at the reference point by  $(\hbar^2/8m) \nabla_{\mathbf{r}}^2 \ell(|\mathbf{r} - \mathbf{r}_i| k_F) \ell(|\mathbf{r} - \mathbf{r}_j| k_F)$ . Finally, one takes the limit of the uniform system, and integrates over the configuration space of the last particle.

Combining Eqs. (2.16) and (2.17) with the potential energy provides us with the starting point for further manipulations,

$$\frac{E}{N} = \frac{T_F}{N} + \frac{\rho}{2} \int d^3r g(r) v_{\text{JF}}(r) + \frac{T_{\text{JF}}}{N}, \quad (2.18)$$

where

$$v_{\text{JF}}(r) = v(r) - \frac{\hbar^2}{4m} \nabla^2 u_2(r) \quad (2.19)$$

is the *Jackson–Feenberg effective interaction*.

#### D. Fermion Euler equations

The formal manipulations to derive an Euler equation for the optimal pair correlations are almost identical to the ones carried out for bosons. The variation with respect to the pair correlation function consists of two terms: One comes from the variation with respect to the pair correlation function  $u_2(r)$  appearing in the Jackson–Feenberg interaction  $v_{\text{JF}}(r)$ , and the second one is due to the variation of the pair distribution function with respect to  $u_2(r)$  and the variation of  $T_{\text{JF}}$ :

$$\frac{\hbar^2}{4m} \nabla^2 g(r) = \int d^3r' v_{\text{JF}}(r') \frac{\delta g(r')}{\delta u_2(r)} + \frac{2}{\rho} \frac{\delta}{\delta u_2(r)} \frac{T_{\text{JF}}}{N} \equiv g'(r). \quad (2.20)$$

The contribution from the first term on the right hand side of Eq. (2.20) to  $g'(r)$  is calculated in complete analogy to the Bose case by replacing, in turn, each correlation line  $\exp[u_2(r_{ij})] - 1$  by  $\exp[u_2(r_{ij})] v_{\text{JF}}(r_{ij})$ . The second term is calculated recalling the graphical construction scheme of  $T_{\text{JF}}$  described above, and applying the same procedure to a graphical expansion of  $g(r)$ . Thus, the contribution to  $g'(r)$  originating from  $T_{\text{JF}}$  is obtained by replacing in  $g(r)$ , in turn, every connected pair of exchange lines  $\ell(r_{ij} k_F) \ell(r_{ik} k_F)$  by  $(\hbar^2/8m) \nabla_i^2 \ell(r_{ij} k_F) \ell(r_{ik} k_F)$ . Following this construction scheme, one derives a set of eight linear equations, the FHNC'–equations, corresponding to the eight FHNC equations (2.7), (2.8) [33], in which the Jackson–Feenberg effective potential and the differentiated exchange functions act as driving terms.

To derive a form of the fermion Euler equations that is useful for a numerical implementation, we write the Euler equation (2.20) in momentum space as

$$\frac{1}{2}t(k)[S(k) - 1] + S'(k) = 0, \quad (2.21)$$

where  $t(k) \equiv \hbar^2 k^2 / 2m$ . The  $S'(k)$  is a linear combination of the non-nodal quantities  $\tilde{X}'_{ij}(k)$

$$S'(k) = \sum_{ij \in \{\text{dd}, \text{de}, \text{ee}\}} \frac{\partial S(k)}{\partial X_{ij}(k)} \tilde{X}'_{ij}(k) \quad (2.22)$$

where the  $\tilde{X}'_{ij}(k)$  are constructed from the non-nodal quantities  $\tilde{X}_{ij}(k)$  analogously to the construction of  $g'(r)$  from  $g(r)$  described above. Next, we define three effective interactions in the dd-, de- and ee-channels as

$$\begin{aligned} \tilde{V}_{\text{dd}}(k) &= \tilde{X}'_{\text{dd}}(k) - \frac{1}{2}t(k)\tilde{X}_{\text{dd}}(k), \\ \tilde{V}_{\text{de}}(k) &= \tilde{X}'_{\text{de}}(k), \\ \tilde{V}_{\text{ee}}(k) &= \tilde{X}'_{\text{ee}}(k) + \frac{1}{2}t(k)\tilde{X}_{\text{ee}}(k). \end{aligned} \quad (2.23)$$

The quantity  $\tilde{V}_{\text{dd}}(k)$ , defined in Eq. (2.23), may be identified with the “direct interaction” of the Babu–Brown theory [43] of the quasiparticle interaction. From Eqs. (2.14), the effective interactions inherit the long-wavelength properties

$$\begin{aligned} \tilde{V}_{\text{de}}(k) &= \mathcal{O}(k) & \text{as } k \rightarrow 0^+, \\ \tilde{V}_{\text{ee}}(k) &= \mathcal{O}(k^2) & \text{as } k \rightarrow 0^+. \end{aligned} \quad (2.24)$$

Using the representation (2.10) for the calculation of  $S'(k)$  via Eq. (2.22) and eliminating the  $X'_{ij}(k)$  in favor of the  $V_{ij}(k)$  lets us rewrite

$$S'(k) = S^2(k)\tilde{V}_{\text{dd}}(k) + 2S(k)S_{\text{d}}(k)\tilde{V}_{\text{de}}(k) + S_{\text{d}}^2(k)\tilde{V}_{\text{ee}}(k) + \frac{1}{2}t(k)[S_{\text{d}}^2(k) - S(k)]. \quad (2.25)$$

Inserting this expression for  $S'(k)$  in the Euler equation (2.21) lets us express  $S(k)$  in terms of the three effective interactions  $\tilde{V}_{ij}(k)$ .

The second step in the derivation of the Euler equation is to eliminate the pair correlation function  $u_2(r)$  by using the FHNC equation (2.7)

$$\begin{aligned} -\frac{\hbar^2}{4m}[1 + \Gamma_{\text{dd}}(r)]\nabla^2 u_2(r) &= -\frac{\hbar^2}{4m}\nabla^2 \Gamma_{\text{dd}}(r) + \frac{\hbar^2}{m}\left|\nabla\sqrt{1 + \Gamma_{\text{dd}}(r)}\right|^2 \\ &+ \frac{\hbar^2}{4m}[1 + \Gamma_{\text{dd}}(r)]\left[\nabla^2 N_{\text{dd}}(r) + \nabla^2 E_{\text{dd}}(r)\right]. \end{aligned} \quad (2.26)$$

Using Eq. (2.26), one can rewrite the effective interactions  $V_{ij}(r)$  in coordinate space entirely in terms of the distribution functions, the yet unspecified sets of elementary diagrams  $E_{ij}(r)$  and their “primed” counterparts  $E'_{ij}(r)$ . The resulting equations are lengthy and not very illuminating; they have been spelled out in Refs. 33 and 34. For the purpose of comparison with the impurity results, we display the coordinate space form of the direct interaction

$$V_{dd}(r) = [1 + \Gamma_{dd}(r)] \left[ v(r) + \frac{\hbar^2}{4m} \nabla^2 E_{dd}(r) + E'_{dd}(r) \right] + \frac{\hbar^2}{m} \left| \nabla \sqrt{1 + \Gamma_{dd}(r)} \right|^2 + \Gamma_{dd}(r) w_I(r), \quad (2.27)$$

$$w_I(r) = \frac{\hbar^2}{4m} \nabla^2 N_{dd}(r) + N'_{dd}(r). \quad (2.28)$$

To calculate the effective interactions  $\tilde{V}_{ij}(k)$  ( $(ij) \in \{dd, de, ee, cc\}$ ) (or  $\tilde{X}'_{ij}(k)$ ) and the fermion analog of the induced potential  $w_I(r)$ , one must also calculate the “primed” analogs of the “nodal” diagrams  $N_{ij}(r)$ . These quantities may be found in Refs. 33 and 34, they are needed for the numerical optimization, but we will not need them in the further discussion. The dd–elementary diagrams have no special features; their omission can cause quantitative changes in the final answer, but does, unlike the de and ee “elementary” diagrams, not change the analytic structure and the properties of the solutions.

### III. IMPURITY CORRELATIONS

In this section, and further on, we also must spell out the particle species, which may be an electron (“background particle”, referred to by a superscript “B”) or a positron (“impurity particle”, referred to by a superscript “I”). It is not necessary to label those quantities that were introduced in the last section and that refer only to background particles. We will keep the formulation general in the sense that the impurity mass  $m_I$  is arbitrary, as well as the interaction between an “impurity” (positron) and a “background” (electron) particle. The Hamiltonian for the full system including the impurity is given by

$$H^I = -\frac{\hbar^2}{2m_I} \nabla_0^2 - \sum_{j=1}^N \frac{\hbar^2}{2m} \nabla_j^2 + \sum_{j=1}^N v^{\text{IB}}(|\mathbf{r}_0 - \mathbf{r}_j|) + \sum_{\substack{j,k=1 \\ j < k}}^N v(|\mathbf{r}_j - \mathbf{r}_k|). \quad (3.1)$$

As a convention, the impurity particle coordinate is  $\mathbf{r}_0$ . In the present case of a positron in an electron gas, the impurity–background interaction  $v^{\text{IB}}(r)$  only differs in the overall sign

from the background–background interaction  $v(r)$ , which is simply the repulsive Coulomb potential. The impurity mass  $m_I$  is equal to the background mass  $m$ , but for a better insight into the problem it is helpful to keep  $m_I$ .

The formulation of the FHNC–EL equations for a single impurity follows essentially the same path as the formulation of the background equations, namely

- Define a variational wave function

$$\Psi_0^{\text{IB}}(0, 1, \dots, N) = \exp \left[ \frac{1}{2} \sum_{i=1}^N u_2^{\text{IB}}(\mathbf{r}_0, \mathbf{r}_i) \right] \Psi_0(1, \dots, N), \quad (3.2)$$

- Derive a set of FHNC equations,
- Derive the corresponding Euler equation using the “prime equation” technique, and
- Reformulate the Euler equation in terms of distribution functions, thereby eliminating any reference to the correlation function  $u_2^{\text{IB}}(r_{ij})$ .

Compared to finite–concentration mixtures, the derivation is simplified because there are no exchanges connected to impurity coordinates.

### A. FHNC equations for one impurity

The (F)HNC technique is well established in earlier work, so there is no need to go through the details of the derivations here. The aspect that distinguishes fermions from bosons are the combinatorial rules and long–wavelength properties discussed above. In a mixture, exchanges can only take place between particles of the same species; this implies in the dilute limit that exchanges occur only between “background” particles. Moreover, in the dilute limit of a mixture *only one* impurity can occur in each diagrammatic quantity.

Since the impurity cannot be involved in any exchange, we have only two FHNC equations: The equations describing the parallel connections between external coordinates are

$$\begin{aligned} \Gamma_{\text{dd}}^{\text{IB}}(r) &= X_{\text{dd}}^{\text{IB}}(r) + N_{\text{dd}}^{\text{IB}}(r) = \exp \left( u_2^{\text{IB}}(r) + N_{\text{dd}}^{\text{IB}}(r) + E_{\text{dd}}^{\text{IB}}(r) \right) - 1, \\ X_{\text{de}}^{\text{IB}}(r) &= \left[ 1 + \Gamma_{\text{dd}}^{\text{IB}}(r) \right] \left[ E_{\text{de}}^{\text{IB}}(r) + N_{\text{de}}^{\text{IB}}(r) \right] - N_{\text{de}}^{\text{IB}}(r) \end{aligned} \quad (3.3)$$

while the chain connections are best written in momentum space,

$$\begin{aligned} \tilde{N}_{\text{dd}}^{\text{IB}}(k) &= (S_{\text{d}}(k) - 1) \tilde{X}_{\text{dd}}^{\text{IB}}(k) + \tilde{\Gamma}_{\text{dd}}(k) \tilde{X}_{\text{de}}^{\text{IB}}(k), \\ \tilde{N}_{\text{de}}^{\text{IB}}(k) &= (S(k) - S_{\text{d}}(k)) \tilde{X}_{\text{dd}}^{\text{IB}}(k) + (S_{\text{d}}(k) - 1 - \tilde{\Gamma}_{\text{dd}}(k)) \tilde{X}_{\text{de}}^{\text{IB}}(k). \end{aligned} \quad (3.4)$$

From these quantities, we can construct the impurity–background distribution function

$$g^{\text{IB}}(r) = \left[1 + \Gamma_{\text{dd}}^{\text{IB}}(r)\right] \left[1 + N_{\text{de}}^{\text{IB}}(r) + E_{\text{de}}^{\text{IB}}(r)\right]. \quad (3.5)$$

The long–wavelength properties corresponding to the identities (2.14) apply only for the background coordinates. Since the exchange structures of  $X_{\text{de}}^{\text{IB}}(r)$  and  $X_{\text{de}}(r)$  are the same, we have the long–wavelength limit

$$\tilde{X}_{\text{de}}^{\text{IB}}(k) = \mathcal{O}(k) \quad \text{as } k \rightarrow 0^+. \quad (3.6)$$

To abbreviate the equations, we found it convenient to define the quantity

$$\tilde{\mathcal{X}}^{\text{IB}}(k) \equiv \tilde{X}_{\text{dd}}^{\text{IB}}(k) + \frac{S_{\text{d}}(k)}{S(k)} \tilde{X}_{\text{de}}^{\text{IB}}(k). \quad (3.7)$$

A few relations are useful in the derivation of the resulting equations:

$$\begin{aligned} S^{\text{IB}}(k) &\equiv \left[g^{\text{IB}}(r) - 1\right]^{\mathcal{F}}(k) = S(k) \tilde{X}_{\text{dd}}^{\text{IB}}(k) + S_{\text{d}}(k) \tilde{X}_{\text{de}}^{\text{IB}}(k) = S(k) \tilde{\mathcal{X}}^{\text{IB}}(k), \\ \tilde{\Gamma}_{\text{dd}}^{\text{IB}}(k) &= S_{\text{d}}(k) \tilde{X}_{\text{dd}}^{\text{IB}}(k) + \tilde{\Gamma}_{\text{dd}}(k) \tilde{X}_{\text{de}}^{\text{IB}}(k) = S_{\text{d}}(k) \tilde{\mathcal{X}}^{\text{IB}}(k) - \frac{\tilde{X}_{\text{de}}^{\text{IB}}(k)}{1 + \tilde{X}_{\text{ee}}(k)}, \\ \tilde{\Gamma}_{\text{dd}}(k) &= \frac{S_{\text{d}}^2(k)}{S(k)} - \frac{1}{1 + \tilde{X}_{\text{ee}}(k)}. \end{aligned} \quad (3.8)$$

## B. Euler equations for one impurity

For the determination of existence and stability of the solutions of the optimization problem, it is again useful to formulate the Euler equation in momentum space; the inclusion of the appropriate classes of “elementary” exchange diagrams always guarantees the proper short–distance behavior. Useful abbreviations are  $t_I(k) = \hbar^2 k^2 / 2m_I$  and the Feynman spectrum of the background,  $\hbar\omega(k) = t(k)/S(k)$ . The formal Euler equation for the impurity–background correlations is [44], in analogy to Eq. (2.21).

$$\frac{1}{4}(t_I(k) + t(k))S^{\text{IB}}(k) + S'^{\text{IB}}(k) = 0. \quad (3.9)$$

The remaining manipulations are to carry out the “priming” operation on the impurity FHNC equations and to formulate the equations in a reasonably plausible form. This can be done in many ways, and the ultimate choice of the formulation depends to some extent

on the iteration path adopted for the numerical solution. Formally, we can define — in analogy to  $\tilde{\mathcal{X}}^{\text{IB}}(k)$  introduced above — and to Eqs. (2.23)

$$\tilde{\mathcal{V}}^{\text{IB}}(k) \equiv \tilde{\mathcal{X}}'^{\text{IB}}(k) - \frac{1}{4}(t(k) + t_I(k))\tilde{\mathcal{X}}^{\text{IB}}(k) \quad (3.10)$$

and rewrite the impurity Euler equation (3.9) as

$$\tilde{\mathcal{X}}^{\text{IB}}(k) = -2 \frac{\tilde{\mathcal{V}}^{\text{IB}}(k)}{t_I(k) + \hbar\omega(k)}. \quad (3.11)$$

This representation of the Euler equation is formally identical to the Euler equation for impurities in Bose liquids. Of course, we still need to derive working formulas for calculating the quantity  $\tilde{\mathcal{V}}^{\text{IB}}(k)$ .

### C. Induced Interactions

From the definitions (3.10) and (3.7), we can write formally

$$\begin{aligned} \tilde{\mathcal{V}}^{\text{IB}}(k) &= \tilde{V}_{\text{dd}}^{\text{IB}}(k) + \frac{S_{\text{d}}(k)}{S(k)}\tilde{V}_{\text{de}}^{\text{IB}}(k) + \left(\frac{S_{\text{d}}(k)}{S(k)}\right)' \tilde{X}_{\text{de}}^{\text{IB}}(k) \\ &= \tilde{V}_{\text{dd}}^{\text{IB}}(k) + \frac{S_{\text{d}}(k)}{S(k)}\tilde{V}_{\text{de}}^{\text{IB}}(k) - \frac{\tilde{X}_{\text{de}}^{\text{IB}}(k)}{1 + \tilde{X}_{\text{ee}}(k)} \left[ \tilde{V}_{\text{de}}(k) + \frac{S_{\text{d}}(k)}{S(k)}\tilde{V}_{\text{ee}}(k) \right] \\ &\quad + \frac{t(k)}{2} \frac{S_{\text{d}}(k)}{S(k)} \frac{\tilde{X}_{\text{de}}^{\text{IB}}(k)\tilde{X}_{\text{ee}}(k)}{1 + \tilde{X}_{\text{ee}}(k)} \end{aligned} \quad (3.12)$$

with (note that we deviate, for convenience and consistency with the definition (3.10) slightly from the definitions (2.23))

$$\begin{aligned} \tilde{V}_{\text{dd}}^{\text{IB}}(k) &= \tilde{X}_{\text{dd}}'^{\text{IB}}(k) - \frac{1}{4}(t_I(k) + t(k))\tilde{X}_{\text{dd}}^{\text{IB}}(k), \\ \tilde{V}_{\text{de}}^{\text{IB}}(k) &= \tilde{X}_{\text{de}}'^{\text{IB}}(k) - \frac{1}{4}(t_I(k) + t(k))\tilde{X}_{\text{de}}^{\text{IB}}(k). \end{aligned} \quad (3.13)$$

The calculation of  $V_{\text{dd}}^{\text{IB}}(r)$  is identical to the one for bosons and mixtures:

$$\begin{aligned} V_{\text{dd}}^{\text{IB}}(r) &= \left[1 + \Gamma_{\text{dd}}^{\text{IB}}(r)\right] \left[v^{\text{IB}}(r) + \Delta V_e^{\text{IB}}(r)\right] \\ &\quad + \left[\frac{\hbar^2}{2m} + \frac{\hbar^2}{2m_I}\right] \left|\nabla \sqrt{1 + \Gamma_{\text{dd}}^{\text{IB}}(r)}\right|^2 + \Gamma_{\text{dd}}^{\text{IB}}(r)w_I^{\text{IB}}(r) \end{aligned} \quad (3.14)$$

with the induced interaction

$$\tilde{w}_I^{\text{IB}}(k) = \tilde{N}_{\text{dd}}'^{\text{IB}}(k) - \frac{1}{4}(t_I(k) + t(k))\tilde{N}_{\text{dd}}^{\text{IB}}(k) \quad (3.15)$$

and the elementary–diagram correction

$$\Delta V_e^{\text{IB}}(r) = \left[ \frac{\hbar^2}{8m} + \frac{\hbar^2}{8m_I} \right] \nabla^2 E_{\text{dd}}^{\text{IB}}(r) + E_{\text{dd}}^{\prime \text{IB}}(r). \quad (3.16)$$

Finally, we need

$$\begin{aligned} V_{\text{de}}^{\text{IB}}(r) &= E_{\text{de}}^{\text{IB}}(r) \left( 1 + \Gamma_{\text{dd}}^{\text{IB}}(r) \right) + \Gamma_{\text{dd}}^{\prime \text{IB}}(r) \left( E_{\text{de}}^{\text{IB}}(r) + N_{\text{de}}^{\text{IB}}(r) \right) \\ &+ \Gamma_{\text{dd}}^{\text{IB}}(r) N_{\text{de}}^{\text{IB}}(r) + \left( \frac{\hbar^2}{8m_I} + \frac{\hbar^2}{8m} \right) \nabla^2 X_{\text{de}}^{\text{IB}}(r), \end{aligned} \quad (3.17)$$

where the de–elementary diagrams must be chosen to guarantee the property  $\tilde{V}_{\text{de}}^{\text{IB}}(k) \rightarrow 0$  as  $k \rightarrow 0^+$ , *cf.* Eq. (3.6).

For the calculation of the remaining ingredients, it is most convenient to start with the effective interaction of correlated basis functions (CBF) theory

$$\tilde{V}_{\text{eff}}^{\text{IB}}(k) = \Gamma_{\text{dd}}^{\prime \text{IB}}(k) - \frac{1}{4}(t_I(k) + t(k))\tilde{\Gamma}_{\text{dd}}^{\text{IB}}(k). \quad (3.18)$$

Again, using background and impurity Euler equations, one can write this quantity as

$$\begin{aligned} \tilde{V}_{\text{eff}}^{\text{IB}}(k) &= -\frac{1}{2} \left[ t_I(k) + \frac{t(k)}{1 + \tilde{X}_{\text{ee}}(k)} \right] \tilde{\Gamma}_{\text{dd}}^{\text{IB}}(k) \\ &- \frac{1}{1 + \tilde{X}_{\text{ee}}(k)} \left[ \tilde{V}_{\text{de}}^{\text{IB}}(k) + S^{\text{IB}}(k)\tilde{V}_{\text{de}}(k) + \tilde{\Gamma}_{\text{dd}}^{\text{IB}}(k)\tilde{V}_{\text{ee}}(k) + \frac{1}{2}(t_I(k) + t(k))\tilde{X}_{\text{de}}^{\text{IB}}(k) \right]. \end{aligned} \quad (3.19)$$

From this, we can obtain, for example, the induced interaction

$$\tilde{w}_I^{\text{IB}}(k) = \tilde{V}_{\text{eff}}^{\text{IB}}(k) - \tilde{V}_{\text{dd}}^{\text{IB}}(k) \quad (3.20)$$

and, of course,  $\tilde{\Gamma}_{\text{dd}}^{\prime \text{IB}}(k)$  which is needed for the *de*–equation, and  $\tilde{N}_{\text{de}}^{\prime \text{IB}}(k)$  which is now easily obtained from

$$\begin{aligned} \tilde{N}_{\text{de}}^{\prime \text{IB}}(k) &= S^{\prime \text{IB}}(k) - \tilde{\Gamma}_{\text{dd}}^{\prime \text{IB}}(k) - \tilde{X}_{\text{de}}^{\prime \text{IB}}(k) \\ &= -\frac{1}{4}(t_I(k) + t(k)) \left( S^{\text{IB}}(k) + \tilde{\Gamma}_{\text{dd}}^{\text{IB}}(k) + \tilde{X}_{\text{dd}}^{\text{IB}}(k) \right) - \tilde{V}_{\text{eff}}^{\text{IB}}(k) - \tilde{V}_{\text{de}}^{\text{IB}}(k). \end{aligned}$$

With this, we have derived a complete set of equations that can be solved by iteration.

#### D. Impurity Energetics

Another physical quantity of interest is the chemical potential of the positron impurity, which is the energy gained or lost by adding one impurity particle into the liquid, *i.e.* the

energy difference

$$\begin{aligned}\mu^I &= E_{N+1} - E_N \\ &= \frac{\langle \Psi^I | H^I | \Psi^I \rangle}{\langle \Psi^I | \Psi^I \rangle} - \frac{\langle \Psi | H | \Psi \rangle}{\langle \Psi | \Psi \rangle}.\end{aligned}\quad (3.21)$$

In the calculation of the impurity chemical potential from the definition (3.21) we must include, besides the explicit terms containing impurity distribution functions, also the *changes* in the background distribution and correlation functions due to the presence of an impurity. These changes are of the order of  $1/N$  and therefore cause a change of order unity in the positron correlation energy. For brevity, we suppress here the contribution from triplet calculations; these corrections are already discussed in Ref. 35. The impurity chemical potential is, at the pair correlation level, given by

$$\begin{aligned}\mu^I &= \rho \int d^3r \left[ [g^{\text{IB}}(r) - 1]v^{\text{IB}}(r) - g^{\text{IB}}(r) \left( \frac{\hbar^2}{8m_I} + \frac{\hbar^2}{8m} \right) \nabla^2 u_2^{\text{IB}}(r) \right] \\ &\quad + \frac{\rho^2 \Omega}{2} \Delta \left\{ \int d^3r \left[ (g(r) - 1)v(r) - \frac{\hbar^2}{4m} g(r) \nabla^2 u_2(r) \right] \right\} + \Delta T_{\text{JF}}\end{aligned}\quad (3.22)$$

where the  $\Delta$ 's in the second line of Eq. (3.22) indicate that we take the difference of the expressions calculated for the full system *minus* the same expression for the pure background.

The pair correlations between background and impurity particles are determined by optimization. Having a relationship between the pair distribution functions  $g^{ij}(r)$  and the pair correlation functions  $u_2^{ij}(r)$  allows us to *choose* which one of these four quantities we consider to be the independent ones. The most convenient choice is to use the “dressed” correlation functions  $\Gamma_{\text{dd}}(r)$  and  $\Gamma_{\text{dd}}^{\text{IB}}(r)$  since all other diagrammatic quantities can be defined in terms of these functions, whereas  $u_2(r)$  appears explicitly only in the coordinate space equation (2.7). In other words, we consider  $u_2(r)$  as a functional of  $\Gamma_{\text{dd}}(r)$ , the impurity density  $\rho^I$ , and  $\rho$ . As mentioned earlier, the consideration is further simplified by the fact that the impurity cannot be involved in any exchange.

Since we need the chemical potential  $\mu^I$  only to leading order in the impurity density, the optimization conditions for the background can be used to simplify the expression (3.22) for the chemical potential (again at the two-body correlation level):

$$\begin{aligned}&\frac{1}{2} \Delta \left\{ \int d^3r_1 d^3r_2 \rho(\mathbf{r}_1, \mathbf{r}_2) \left[ V(|\mathbf{r}_1 - \mathbf{r}_2|) - \frac{\hbar^2}{8m} (\nabla_1^2 + \nabla_2^2) u_2(\mathbf{r}_1, \mathbf{r}_2) \right] \right\} \\ &= -\frac{1}{2} \int d^3r_1 d^3r_2 \rho(\mathbf{r}_1, \mathbf{r}_2) \frac{\hbar^2}{8m} (\nabla_1^2 + \nabla_2^2) \Delta u_2(\mathbf{r}_1, \mathbf{r}_2).\end{aligned}\quad (3.23)$$



In particular, since  $T_{\text{JF}}$  can be expressed entirely in terms of the  $\Gamma_{\text{dd}}(r_{ij})$  and exchange functions, there is no rearrangement correction from this term. The change,  $\Delta u_2$ , is now expressed as a functional of the impurity quantities,

$$\begin{aligned}\Delta u_2(r) &\equiv \Delta u_2[\rho^I, g^{\text{IB}}, u_2^{\text{IB}}] \\ &= \int d^3 r_0 \rho^I \frac{\delta u_2(\mathbf{r}_1, \mathbf{r}_2)}{\delta \rho^I}.\end{aligned}\tag{3.24}$$

Furthermore using the HNC equation we find, again in HNC approximation, that

$$\Delta u_2(\mathbf{r}_1, \mathbf{r}_2) = - \int d^3 r_0 \rho^I \frac{\delta N_{\text{dd}}(\mathbf{r}_1, \mathbf{r}_2)}{\delta \rho^I}.\tag{3.25}$$

The variations are carried out for *fixed pair distribution functions*. The change in the sum of nodal diagrams has a simple expression in the momentum space,

$$\rho^I \frac{\delta \tilde{N}_{\text{dd}}(k)}{\delta \rho^I} = \left( \tilde{X}_{\text{dd}}^{\text{IB}}(k) \right)^2.\tag{3.26}$$

The HNC equations (2.7) and (3.3) are now used to eliminate the pair correlation functions  $u_2(r)$  and  $u_2^{\text{IB}}(r)$  from the chemical potential (3.22). Using the HNC equations and Eq. (3.26) one finds after some algebraic manipulations

$$\begin{aligned}\mu_{\text{HNC}}^I &= \rho \int d^3 r \left[ g^{\text{IB}}(r) v^{\text{IB}}(r) + \left[ \frac{\hbar^2}{2m_I} + \frac{\hbar^2}{2m} \right] \left| \nabla \sqrt{g^{\text{IB}}(r)} \right|^2 \right] \\ &+ \frac{1}{4} \int \frac{d^3 k}{(2\pi)^3 \rho} [t(k) + t_I(k)] \left[ S^{\text{IB}}(k) \left[ \tilde{N}_{\text{dd}}^{\text{IB}}(k) + \tilde{E}_{\text{dd}}^{\text{IB}}(k) \right] - \left[ \tilde{N}_{\text{de}}^{\text{IB}}(k) + \tilde{E}_{\text{de}}^{\text{IB}}(k) \right] \tilde{\Gamma}_{\text{dd}}^{\text{IB}}(k) \right] \\ &+ \frac{1}{4} \int \frac{d^3 k}{(2\pi)^3 \rho} t(k) [S(k) - 1] \left[ \tilde{X}_{\text{dd}}^{\text{IB}}(k) \right]^2.\end{aligned}\tag{3.27}$$

The expression given above must be supplemented by corrections originating from “proper” elementary diagrams and triplet correlations (see Ref. 35) if appropriate.

#### IV. SIMPLIFICATIONS

The FHNC–EL equations for the background, and even more for the impurity, are admittedly complicated and of little appeal. The reason is that the exchange structure allows for many different ways of coupling.

We recall, however, that the original motivation for deriving these equations is a symmetric treatment of short– and long– ranged correlations, and the stability criteria provided by the optimization. One is therefore tempted to reduce the FHNC–EL equations to a level that

contains the *minimal* amount of self-consistency and is, nevertheless, optimizeable. An appealing feature of such a simplified theory is that the equations are hardly more complicated than those of the Bose theory; they are also readily applied to the much more demanding problem of inhomogeneous systems, where the solution of the full set of FHNC–EL equations is a rather unpleasant and still uncompleted task [45]. In this connection, we need to recall two things: First, positron annihilation rates are directly connected to short-ranged correlations, *c.f.* Eq. (1.1). Second, it is far from straightforward to deduce short-ranged correlations in an inhomogeneous geometry from results on the homogeneous electron gas [46].

### A. FHNC//0 for the background

The FHNC//0 approximation is, by construction, the *minimum* approximation that is (a) correct for both short- and long-range correlations and (b) permits optimization. The FHNC//0 approximation for the background amounts to ignoring all *de* quantities and using  $1 + \tilde{X}_{ee}(k) = S_F(k)$ , where

$$S_F(k) = \begin{cases} \frac{3k}{4k_F} - \frac{k^3}{16k_F^2} & k < 2k_F \\ 1 & k \geq 2k_F \end{cases} \quad (4.1)$$

is the static structure function of the non-interacting Fermi gas.

Consistent with this approximation, we leave out “elementary” diagrams; they may be put in at the end on a term-by-term basis. The FHNC equations (2.7), (2.8) collapse to three equations:

$$\begin{aligned} X_{dd}(r) &= \exp[u_2(r) + N_{dd}(r)] - 1 - N_{dd}(r), \\ \tilde{N}_{dd}(k) &= \frac{\tilde{X}_{dd}(k)}{1 - S_F(k)\tilde{X}_{dd}(k)}, \\ S(k) &= \frac{S_F(k)}{1 - S_F(k)\tilde{X}_{dd}(k)}. \end{aligned} \quad (4.2)$$

Eqs. (4.2) are exact in the long-wavelength limit, but can be applied also at finite momenta.

In the same approximation, we obtain from Eq. (2.21)

$$S(k) = \frac{S_F(k)}{\sqrt{1 + 2\frac{S_F^2(k)}{t(k)}\tilde{V}_{p-h}(k)}},$$

$$\begin{aligned}
V_{\text{dd}}(r) &= [1 + \Gamma_{\text{dd}}(r)] v(r) + \frac{\hbar^2}{m} \left| \nabla \sqrt{1 + \Gamma_{\text{dd}}(r)} \right|^2 + \Gamma_{\text{dd}}(r) w_{\text{I}}(r), \\
\tilde{w}_{\text{I}}(k) &= -\frac{\hbar^2 k^2}{4m} \left[ \frac{1}{S_{\text{F}}(k)} - \frac{1}{S(k)} \right]^2 \left[ 2 \frac{S(k)}{S_{\text{F}}(k)} + 1 \right].
\end{aligned} \tag{4.3}$$

For further reference, we also mention that, in the same approximation,

$$\tilde{\Gamma}'_{\text{dd}}(k) = \frac{1}{2} t(k) \tilde{\Gamma}_{\text{dd}}(k) \left[ 1 - \frac{2}{S_{\text{F}}(k)} \right]. \tag{4.4}$$

### B. FHNC//0 for the impurity

Leaving the FHNC equations of section III A unchanged but identifying  $1 + \tilde{X}_{\text{ee}}(k) = S_{\text{F}}(k)$  and  $S(k)/S_{\text{d}}(k) = S_{\text{F}}(k)$  and ignoring  $\tilde{V}_{\text{de}}(k)$  and  $\tilde{V}_{\text{ee}}(k)$ , the impurity Euler equations reduce to

$$\tilde{\mathcal{V}}^{\text{IB}}(k) = \tilde{V}_{\text{dd}}^{\text{IB}}(k) + \frac{\tilde{V}_{\text{de}}^{\text{IB}}(k)}{S_{\text{F}}(k)} - \frac{t(k)}{2} \frac{\tilde{X}_{\text{de}}^{\text{IB}}(k)}{S_{\text{F}}^2(k)} [S_{\text{F}}(k) - 1]. \tag{4.5}$$

The induced interaction is

$$\begin{aligned}
\tilde{w}_{\text{I}}^{\text{IB}}(k) &= -\frac{1}{2} \left[ t_{\text{I}}(k) + \frac{t(k)}{S_{\text{F}}(k)} \right] \tilde{\Gamma}_{\text{dd}}^{\text{IB}}(k) - \frac{1}{S_{\text{F}}(k)} \left[ \tilde{V}_{\text{de}}^{\text{IB}}(k) - \frac{1}{2} [t_{\text{I}}(k) + t(k)] \tilde{X}_{\text{de}}^{\text{IB}}(k) \right] \\
&\quad - \tilde{V}_{\text{de}}^{\text{IB}}(k).
\end{aligned} \tag{4.6}$$

The  $de'$ -equation does not simplify significantly, note especially that it is not legitimate to omit the “elementary” exchange diagrams.

Let us finally also ignore all impurity  $de$  quantities. The Euler equation (3.11) remains the same, we only need to replace  $\mathcal{X}^{\text{IB}} \rightarrow X_{\text{dd}}^{\text{IB}}$  and  $\mathcal{V}^{\text{IB}} \rightarrow V_{\text{dd}}^{\text{IB}}$ . We can write it also as

$$S^{\text{IB}}(k) = -2 \frac{S(k) \tilde{V}_{\text{dd}}^{\text{IB}}(k)}{t_{\text{I}}(k) + \hbar \omega(k)}, \tag{4.7}$$

$$V_{\text{dd}}^{\text{IB}}(r) = \frac{\hbar^2}{m} \left| \nabla \sqrt{1 + \Gamma_{\text{dd}}^{\text{IB}}(r)} \right|^2 + \left( 1 + \Gamma_{\text{dd}}^{\text{IB}}(r) \right) v^{\text{IB}}(r) + \Gamma_{\text{dd}}^{\text{IB}}(r) w_{\text{I}}^{\text{IB}}(r). \tag{4.8}$$

The induced interaction is

$$\begin{aligned}
\tilde{w}_{\text{I}}^{\text{IB}}(k) &= -\tilde{V}_{\text{dd}}^{\text{IB}}(k) - \frac{1}{2} \left[ \frac{t(k)}{S_{\text{F}}(k)} + t_{\text{I}}(k) \right] \tilde{\Gamma}_{\text{dd}}^{\text{IB}}(k) \\
&= \frac{1}{2} S^{\text{IB}}(k) \left( \frac{t(k)}{S^2(k)} - \frac{t(k)}{S_{\text{F}}^2(k)} + \frac{t_{\text{I}}(k)}{S(k)} - \frac{t_{\text{I}}(k)}{S_{\text{F}}(k)} \right)
\end{aligned} \tag{4.9}$$

and finally

$$\tilde{\Gamma}_{\text{dd}}^{\text{IB}}(k) = \frac{S^{\text{IB}}(k)}{S_F(k)}. \quad (4.10)$$

We can apply the above sequence of simplifications in two ways: One way is to use the FHNC//0 approximation for the background only, keeping all impurity equations intact. This might be a possible strategy for calculating annihilation rates in inhomogeneous geometries, the good agreement between the  $g^{\text{IB}}(0)$  values in this approximation with the Monte Carlo data of Ortiz [47] provides encouragement that this is perhaps a pragmatic way to attack this problem.

The second level of approximation is to also omit the  $de$ -diagrams in the impurity equations. We note that *both* strategies include the self-consistent summation of ring- and ladder- diagrams [48, 49], *both* strategies also maintain “perfect screening”  $S^{\text{IB}}(k) = 1$ . The FHNC//0 approximation provides for bulk electrons an accuracy that is only marginally worse than the full theory [45], and one might hope that the same is true for electron-positron mixtures. However, since the above approximation omits the self-consistent summation of “elementary” exchange diagrams, the pair distribution function and the structure function become inconsistent. A simple approximation for  $g^{\text{IB}}(r)$  would be

$$g^{\text{IB}}(r) \approx 1 + \Gamma_{\text{dd}}^{\text{IB}}(r). \quad (4.11)$$

Adding the simplest exchange term would lead to a different approximation,

$$g^{\text{IB}}(r) \approx [1 + \Gamma_{\text{dd}}^{\text{IB}}(r)] [1 + C(r)], \quad (4.12)$$

where  $\tilde{C}(k) = \tilde{\Gamma}_{\text{dd}}^{\text{IB}}(k) [S_F(k) - 1]$ . This is acceptable in a system with repulsive interactions since  $1 + \Gamma_{\text{dd}}^{\text{IB}}(r)$  is small at the origin. However, the opposite is true for the electron-positron case because both  $g^{\text{IB}}(r)$  and  $1 + \Gamma_{\text{dd}}^{\text{IB}}(r)$  become large at the origin, thus enhancing any small error that might be made in calculating the exchange corrections. We will see in the next section that this effect can be quite dramatic.

## V. ANNIHILATION RATES

The central quantity of interest of our calculation is the positron annihilation rate (1.1), hence, our primary question is *what does it take to get  $\tau$  right ?* To examine this question, we have carried out the following sequence of calculations of increasing complexity:

- Charged bosons: Positive impurity in a charged Bose gas.
- FHNC//0 : The basic version of the FHNC–EL theory for both the background and the impurity. This means we use Eqs. (4.2)–(4.4) for the background, and Eqs. (4.7)–(4.10) for the impurity. The motivation for this approximation is that it is the simplest one that contains fermionic corrections, satisfies all exact short– and long–wavelength properties, and can therefore be optimized.
- FHNC//0b: The full impurity FHNC–EL equations on the simplified background. The motivation for this approximation is that there is evidence that a simplified treatment of the background electrons could be appropriate, in fact, the energetics of the bulk electron gas predicted by this approximation is not significantly worse than the energetics produced by the full theory [45]. However, electrons and positrons are strongly correlated and, thus, the same approximation might not be adequate for electron–positron correlations. Since the treatment of the impurity correlations is identical to the one of the full FHNC–EL theory to be described below, the comparison of the results from this calculation with the ones from the next more sophisticated one examines the sensitivity of the results to the background correlations.
- FHNC//C0 : The full solution of the FHNC–EL equations for the electrons and the positronic impurity, including corrections that guarantee the long–wavelength limit (3.6) but *without* proper elementary diagrams.
- FHNC//C5 : As FHNC//C0, but including 4<sup>th</sup> and 5<sup>th</sup> order proper elementary diagrams as described in Ref. 34.

Table I lists a comparison of our results for the primary quantity,  $g^{\text{IB}}(0)$ , in the simplest charged boson calculation (see also Ref. 25), our most sophisticated FHNC//C5 calculation, and a few important earlier calculations [8, 19, 24, 26, 47]. At high densities, one has reasonable agreement whereas the agreement becomes worse at lower densities. The comparison of different methods should serve to identify the source of these discrepancies. Among the various calculations, the variational Monte Carlo calculations of Ortiz [47] have produced consistently the lowest values for  $g^{\text{IB}}(0)$ ; incidentally, these values are quite close to our FHNC//0b results.

$r_s$	Kahana	BSS	Lantto	SL	Ortiz	Bosons	FHNC//C5
1			2.16	2.29	2.06	2.40	2.076
2	2.21	3.76	4.05	3.96	3.39	4.55	3.983
3	2.67	6.91	7.40	7.29	7.00	8.25	7.658
4	3.17	13.6	13.2	13.6	11.70	14.71	14.455
5			23.0	24.2	17.69	26.08	26.225
6				40.1		46.18	45.640
8				93.9	64.00	143.30	126.063

TABLE I: The table compares the primary quantity of interest,  $g^{\text{IB}}(0)$ , for the “charged boson” approximation (Bosons) and the FHNC//C5 approximation, with the values obtained by Kahana [8], Boroński, Szotek and Stachowiak (BSS) [19], Lantto [24], Stachowiak and Lach (SL) [26], and Ortiz [47].

Fig. 1 shows the annihilation rates  $\tau^{-1}$  computed using the approximations listed above. More appropriately, one should refer to these numbers as “partial annihilation rates” because we have neglected the effect of core electrons. Sob [50] obtains, for example, 5% core contribution for Li, and 30 % for Cs, whereas more recent work [51, 52] arrives at even larger core corrections. We conclude first that, in the experimentally accessible density range, the “charged boson” approximation is not as bad as one might expect. Inclusion of the simplest fermion corrections (FHNC//0) yields, on the other hand, far too high annihilation rates. This failure is rather surprising, because the approximation already includes the self-consistent summation of both ring and ladder diagrams [48, 49], and is thus beyond standard perturbative treatments that include only one of the classes of diagrams or an incomplete self-consistency scheme.

The main reason for the failure of the FHNC//0 approximation can be traced to the way exchange corrections were included (see the discussion in the end of section IV). On the level FHNC//0b this problem is solved by including the full FHNC summation for the impurity correlations, while leaving the background correlations at the FHNC//0 level. Indeed, there is some improvement. The annihilation rates come out lower than those predicted by the more sophisticated approaches to be discussed below. But, in fact, when core corrections

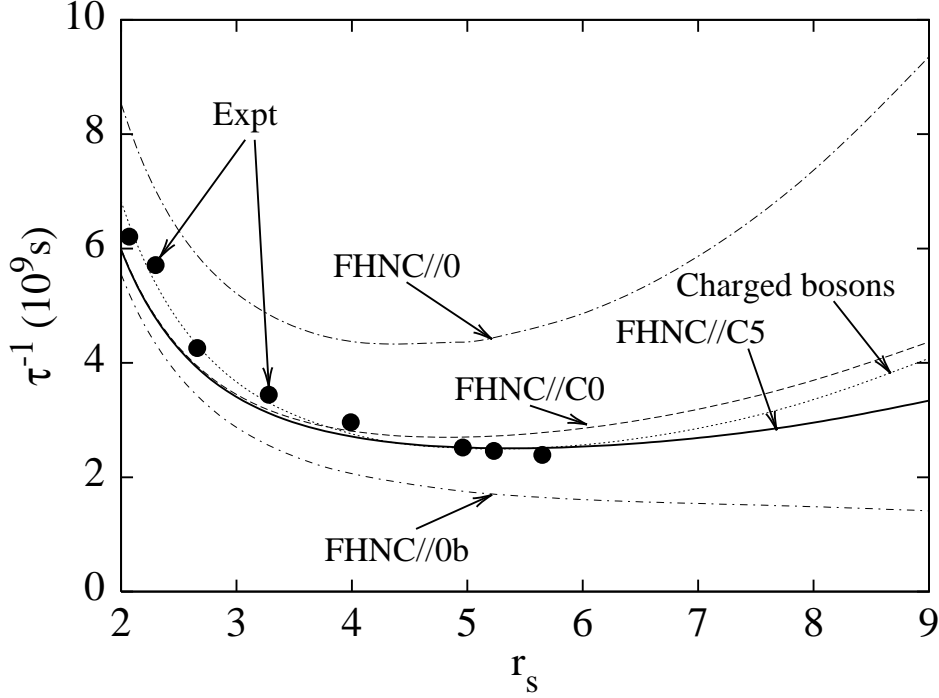


FIG. 1: Experimental and theoretical annihilation rates for various materials. The experimental points are, from left to right, for the metals Al, Zn, Mg, Li, Na, K, Rb, and Cs [4, 53, 54], without core corrections. The theoretical curves correspond to various levels of implementation of the (F)HNC–EL theory as labeled in the figure. In the level of sophistication the order from simple to complex is: Charged bosons, FHNC//0, FHNC//0b, FHNC//C0, FHNC//C5 (see main text for definitions). The positronium decay rate is  $(500 \text{ ps})^{-1} = 2 \times 10^9 \text{ s}^{-1}$ .

are included, agreement of the FHNC//0b approximation with experiments is not too bad. The full FHNC summation FHNC//C0 brings us back up, and ultimately the inclusion of “proper” elementary diagrams on level FHNC//C5 produces reasonable agreement with the experimental annihilation rates when core corrections are omitted.

Evidently  $g^{\text{IB}}(0)$  is extremely sensitive to the description of the background electron liquid, as can be seen in the large difference between the full FHNC//0, the FHNC//0b and the FHNC//C0 results. We conclude therefore that any simplistic treatment of background correlations should be viewed with much reservation.

In discussing the possible theoretical refinements one should finally comment on the importance of triplet correlations. Since the proper elementary diagrams have an impact, one might expect the same to be true for triplets as well. In the case of helium liquids,

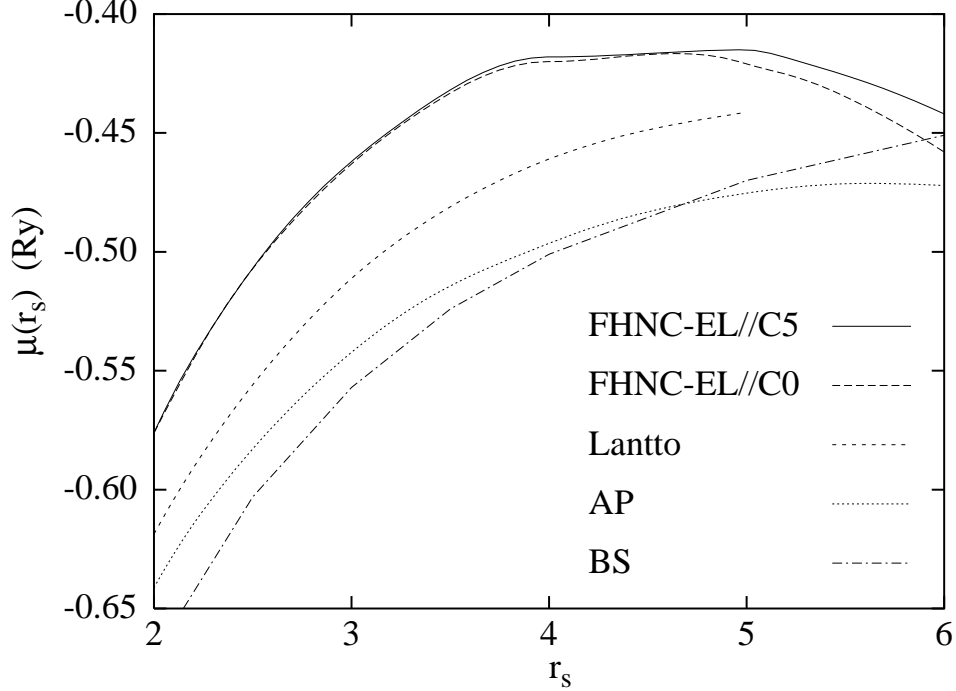


FIG. 2: The calculated positron correlation energies as function of  $r_s$  in the FHNC//C0 (dashed line) and the FHNC//C5 (solid line) approximation. Also shown are the theoretical results of Lantto [24], Arponen and Pajanne (AP) [9], and Boroński and Stachowiak (BS) [31].

triplets have been mostly described in the “convolution approximation” outlined in Ref. 44. Recently, the treatment has also been found to be adequate for a problem analogous to the present one, namely the calculation of the energetics of a  $^4\text{He}$  impurity in  $^3\text{He}$  [35]. The next systematic improvement to the method of Ref. 44 has also been examined [55], but for helium liquids it was found to be insignificant. Unfortunately, the same is not true for positronic impurities in the electron gas. We have tried the same approach here and found that the “convolution approximation” is manifestly inadequate for this case. It appears that the derivation of triplet HNC equations [56] is necessary for a satisfactory treatment. We are not aware of a successful implementation of this program for bosons, much less for fermions or mixtures, and must leave this question open for the time being. The variational Monte Carlo calculations of Ortiz [47] support our view that triplet correlations are unimportant.

From now on we show only the FHNC//C5 result, and occasionally the FHNC//0 result for reference. The next quantity of interest is the positron correlation energy (or chemical potential) (3.21). Our results are shown in Fig. 2; they are consistent with earlier calcula-



tions of Arponen and Pajanne [9] and Lantto [24], although our results are somewhat higher. The present results also show a drop of the chemical potential towards lower densities; a similar drop has been reported by Hodges and Stott [57].

It has been argued that, in the low-density limit (large  $r_s$ ), the correlation energy should go towards the binding energy of the free positronium of -0.524 eV. Evidently, our calculation does not show such an asymptotic behavior and we hasten to point out that it should not: The Jastrow-Feenberg function used in Eqs. (2.2) and (3.2) describes a state in which the positron is delocalized, so it is *not* a valid description of one positronium atom and  $N$  free electrons. Hence, the present theory is inapplicable to a system with bound electron-positron pairs. It has, however, the desirable feature that the Euler equation ceases to have a solution at the point where system cannot be in the state described by the trial wave function. In the present case, this happens at the density where the positron *must* be localized. This feature of the theory does not preclude that the free positronium is the physical low-density limit; the theory simply makes no statement about this limit.

The appearance of a positronium atom is, on one hand, signaled by a very large  $g^{\text{IB}}(0)$ . Moreover, recall that we solve the Euler equation with the boundary condition  $g^{\text{IB}}(r) \rightarrow 1$ , as  $r \rightarrow \infty$ . If there were a bound state, then  $\sqrt{g^{\text{IB}}(r)}$  should have a node at some finite distance. Of course — as argued above — the theory will not allow us to reach this point, but one should expect precursor phenomena as one approaches the density of positronium formation. Fig. 3 shows indeed both effects: As we decrease the density, the  $g^{\text{IB}}(0)$  increases. In addition to this, a “dip” forms at an intermediate distance. At the highest  $r_s$  value shown in Fig. 3,  $r_s = 9$ , we have  $g^{\text{IB}}(r)$  as low as 0.042. With decreasing density the dip drops rapidly, and finally the pair distribution function becomes unphysically negative at  $r_s \approx 9.4$ . Also  $g^{\text{IB}}(0)$  diverges, at  $r_s = 10$ , but because of both diagrammatic approximations and numerical limitations one cannot expect these instabilities to show up at exactly the same density. We conclude that our calculations predict positronium formation at  $9.4 \leq r_s \leq 10$ . For comparison, in the mid 70’s Lowy and Jackson [18] found the positronium limit at  $r_s \geq 6.2$ , while a decade later Pietiläinen and Kallio [23] obtained  $r_s \geq 8$ .

Slightly different information is contained in the static electron-positron structure function  $S^{\text{IB}}(k)$ , depicted in Fig. 4. In the long wavelength limit, charge conservation implies  $S^{\text{IB}}(0+) = 1$ ; this property is a rigorous feature of the optimized structure function in any level of the FHNC-EL approximations. As the density decreases, we see that  $S^{\text{IB}}(k)$  de-

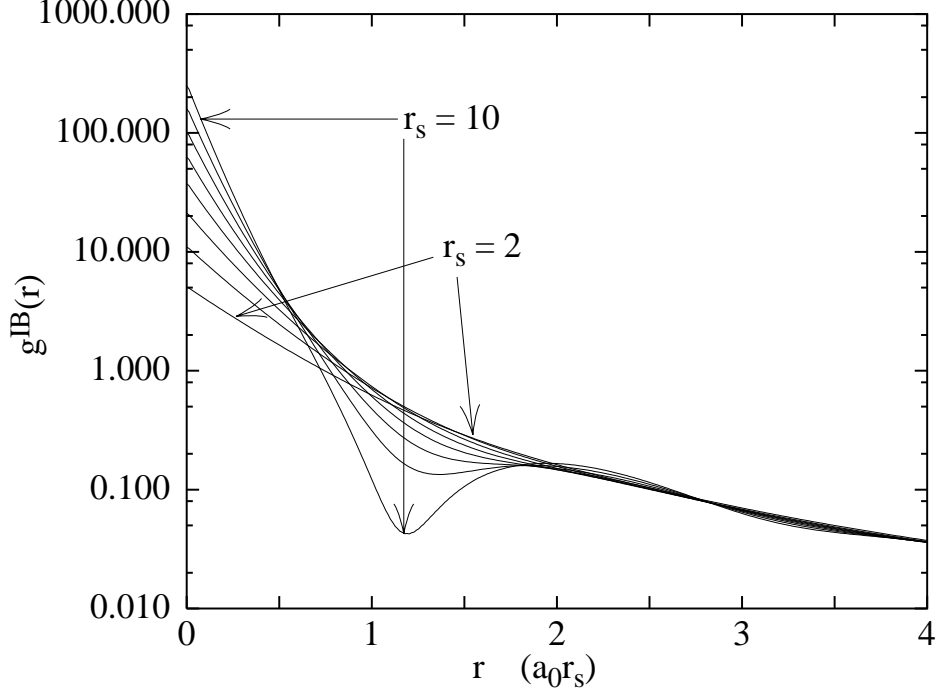


FIG. 3: The figure shows our calculated electron–positron pair distribution function  $g^{\text{IB}}(r)$  for  $r_s = 1, 2, \dots, 9$ . The function with the lowest value of  $g^{\text{IB}}(0)$  corresponds to the highest electron density. Notice the logarithmic scale in  $g^{\text{IB}}(r)$ .

velops a peak at  $k \approx 3.2(a_0 r_s)^{-1}$ . Such a peak reflects an oscillatory structure in the pair distribution function.

## VI. SUMMARY

We have presented in this work calculations of electron–positron correlations in simple metals. Technically, we have used the most complete summation of diagrams within the Jastrow–Feenberg theory. We have shown that such a highly summed theory is indeed necessary for a reasonably reliable prediction of the relevant quantities. The omission of triplet correlations is an unsatisfactory point, but progress towards a fully consistent summation of three–body (F)HNC equations and the corresponding Euler equation is not in sight. In any event, we have demonstrated that one might have to do even more, but one must definitely not do less than was done in our work to obtain a conclusive answer.

Our results are, from a pragmatic point of view, somewhat disappointing in the sense

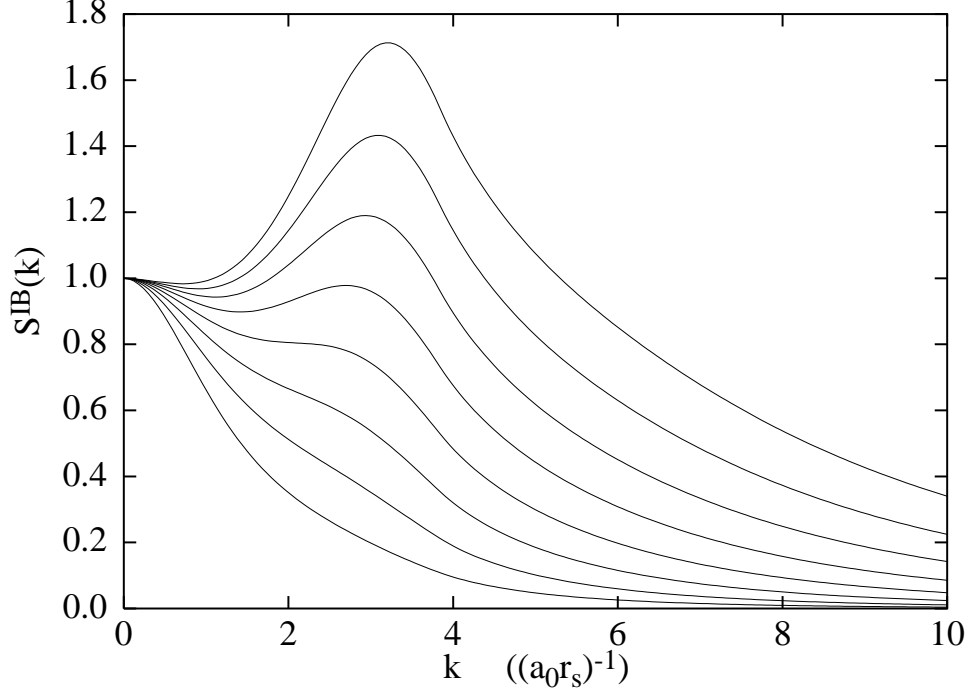


FIG. 4: The figure shows our calculated electron–positron structure function  $S^{\text{IB}}(k)$  for  $r_s = 2, 3, \dots, 9$ . The lowest curve corresponds to the lowest  $r_s$  (highest electron density).

that the system is evidently much more complicated than the bulk electron gas at metallic densities. Bulk electrons at metallic densities are one of the simplest systems to be treated within microscopic many–body theory, and simple approximation provide already reasonable agreement with exact results. The reason for this problem is evidently the large value of the pair–distribution function at the origin, which causes poor convergence of diagrammatic summations. On the other hand, the FHNC//0b approximation seems to provide reasonable agreement with experiments when core–corrections are included. With sufficient caution, since better agreement with experiments does not indicate a better theoretical treatment, one might be able to use this version of the theory in a non–uniform environment and obtain reasonable annihilation rates for positrons in simple metal surfaces [45].

### Acknowledgments

This work was supported, in part, by the Austrian Science Fund under project P12832–TPH. Extensive discussions and communications with H. Sormann and the communication

of unpublished results by G. Ortiz are gratefully acknowledged

- 
- [1] C. Itzykson and J.-B. Zuber, *Quantum Field Theory* (McGraw-Hill Inc., New York, 1980).
  - [2] J. Jauch and F. Rohrlich, *The Theory of Photons and electrons* (Springer-Verlag, New York Heidelberg Berlin, 1976).
  - [3] G. G. Rydzhikh and J. Mitroy, Phys. Rev. Lett. **79**, 4124 (1997).
  - [4] H. Weisberg and S. Berko, Phys. Rev. **154**, 154 (1967).
  - [5] R. A. Ferrell, Rev. Mod. Phys. **28**, 308 (1956).
  - [6] W. Brandt, in *Proceedings of the International School of Physics “Enrico Fermi”, Course LXXXIII*, edited by W. Brandt and A. Dupasquier (North-Holland, Amsterdam, New York, Oxford, 1983), pp. 1–31.
  - [7] B. Barbiellini, M. J. Puska, T. Korhonen, A. Harju, T. Torsti, and R. M. Nieminen, Phys. Rev. B **53**, 16201 (1996).
  - [8] S. Kahana, Phys. Rev. B **129**, 1622 (1963).
  - [9] J. Arponen and E. Pajanne, Ann. Phys. **121**, 343 (1979).
  - [10] H. Sormann, Phys. Rev. B **54**, 4558 (1996).
  - [11] J. Mitroy and B. Barbiellini, Phys. Rev. B **65**, 235103 (2002).
  - [12] H. Stachowiak and E. Boroński, Phys. Rev. B **64**, 195116 (2001).
  - [13] R. A. Ferrell, Phys. Rev. **108**, 167 (1957).
  - [14] E. Boroński and R. M. Nieminen, Phys. Rev. B **34**, 3820 (1986).
  - [15] M. J. Puska and R. M. Nieminen, Rev. Mod. Phys. **66**, 841 (1994).
  - [16] E. Bonderup, J. U. Andersen, and D. N. Lowy, Phys. Rev. B **20**, 883 (1979).
  - [17] D. N. Lowy and G. E. Brown, Phys. Rev. B **12**, 2138 (1975).
  - [18] D. N. Lowy and A. D. Jackson, Phys. Rev. B **12**, 1689 (1975).
  - [19] E. Boroński, Z. Szotek, and H. Stachowiak, Physical-Review-B-Condensed-Matter **23(4)**, 1785 (1981).
  - [20] A. Rubaszek and H. Stachowiak, Phys. Status Solidi B **124**, 159 (1984).
  - [21] A. Rubaszek and H. Stachowiak, Phys. Rev. B **38**, 3846 (1988).
  - [22] A. Kallio, P. Pietiläinen, and L. J. Lantto, Phys. Scr. **25**, 943 (1982).
  - [23] P. Pietiläinen and A. Kallio, Phys. Rev. B **27**, 224 (1983).
  - [24] L. J. Lantto, Phys. Rev. B **36**, 5160 (1987).

- [25] A. Kallio, V. Apaja, and S. Pöykkö, in *Recent Progress in Many Body Theories*, edited by E. Schachinger, H. Mitter, and H. Sormann (Plenum, New York, 1995), vol. 4, pp. 381–391.
- [26] H. Stachowiak and J. Lach, Phys. Rev. B **48**, 9828 (1993).
- [27] J. Gondzik and H. Stachowiak, J. Phys. C: Solid State Phys. **18**, 5399 (1985).
- [28] H. Stachowiak, Phys. Rev. B **41**, 12522 (1990).
- [29] H. Stachowiak, E. Boroński, and G. Banach, Phys. Rev. B **62**, 4431 (2000).
- [30] H. Stachowiak, Phys. Rev. B **56**, 4545 (1997).
- [31] E. Boroński and H. Stachowiak, Phys. Rev. B **57**, 6215 (1998).
- [32] E. Krotscheck and M. L. Ristig, Phys. Lett. A **48**, 17 (1974).
- [33] E. Krotscheck, Ann. Phys. (NY) **155**, 1 (1984).
- [34] E. Krotscheck, J. Low Temp. Phys. **119**, 103 (2000).
- [35] V. Apaja, E. Krotscheck, and J. Springer, J. Low Temp. Phys. **132**, 167 (2003).
- [36] E. Feenberg, *Theory of Quantum Fluids* (Academic, New York, 1969).
- [37] V. Apaja, J. Halinen, V. Halonen, E. Krotscheck, and M. Saarela, Phys. Rev. B **55**, 12925 (1997).
- [38] Y. Kwon, D. M. Ceperley, and R. M. Martin, Phys. Rev. B **58**, 6800 (1998).
- [39] J. W. Clark, in *Progress in Particle and Nuclear Physics*, edited by D. H. Wilkinson (Pergamon Press Ltd., Oxford, 1979), vol. 2, pp. 89–199.
- [40] S. Fantoni and S. Rosati, Nuovo Cimento **25A**, 593 (1975).
- [41] J. G. Zabolitzky, Phys. Rev. A **16**, 1258 (1977).
- [42] E. Krotscheck, Phys. Rev. A **15**, 397 (1977).
- [43] S. Babu and G. E. Brown, Ann. Phys. (NY) **78**, 1 (1973).
- [44] E. Krotscheck and M. Saarela, Physics Reports **232**, 1 (1993).
- [45] E. Krotscheck, W. Kohn, and G.-X. Qian, Phys. Rev. B **32**, 5693 (1985).
- [46] E. Krotscheck and W. Kohn, Phys. Rev. Lett. **57**, 862 (1986).
- [47] G. Ortiz, Ph.D. thesis, Ecole Polytechnique Fédérale de Lausanne (1992).
- [48] A. D. Jackson, A. Lande, and R. A. Smith, Physics Reports **86**, 55 (1982).
- [49] A. D. Jackson, A. Lande, and R. A. Smith, Phys. Rev. Lett. **54**, 1469 (1985).
- [50] M. Sob, Solid Stat. Commun. **53**, 249 (1985).
- [51] S. Daniuk, M. Sob, and A. Rubaszek, Phys. Rev. B **43**, 2580 (1991).
- [52] M. Alatalo, B. Barbiellini, M. Hakala, H. Kauppinen, T. Korhonen, M. J. Puska, K. Saarinen,

- P. Hautojärvi, and R. M. Nieminen, Phys. Rev. B **54**, 2397 (1996).
- [53] A. Seeger, J. Phys. F **3**, 248 (1973).
- [54] T. M. Hall, Phys. Rev. B **10**, 3062 (1974).
- [55] E. Krotscheck, Phys. Rev. B **33**, 3158 (1986).
- [56] M. S. Wertheim, J. Math. Phys **8**, 927 (1967).
- [57] C. H. Hodges and M. J. Stott, Phys. Rev. B **7**, 73 (1973).